Hindawi Publishing Corporation
International Journal of Photoenergy
Volume 2011, Article ID 969214, 5 pages
doi:10.1155/2011/969214

Research Article

Preparation and Characterization of Coevaporated $Cd_{1-x}Zn_xS$ Alloy Thin Films

Wei Li, Jiayi Yang, Zhen Sun, Lianghuan Feng, Jingquan Zhang, and Lili Wu

College of Materials Science and Engineering, Sichuan University, Chengdu 610064, China

Correspondence should be addressed to Wei Li, waylee2000@sohu.com

Received 30 April 2011; Accepted 30 August 2011

Academic Editor: Leonardo Palmisano

$Cd_{1-x}Zn_xS$ thin films have been prepared by the vacuum coevaporation method. The structural, compositional, and optical properties of $Cd_{1-x}Zn_xS$ thin films have been investigated using X-ray diffraction, X-ray fluorescence, and optical transmittance spectra. As-deposited $Cd_{1-x}Zn_xS$ thin films are polycrystalline and show the cubic structure for $x = 1$ and hexagonal one for $x < 1$ with the highly preferential orientation. The composition of $Cd_{1-x}Zn_xS$ thin films determined from Vegard's law and quartz thickness monitors agrees with that determined from the X-ray fluorescence spectra. Optical absorption edge of optical transmittance for $Cd_{1-x}Zn_xS$ thin films shows a blue shift with the increase of the zinc content. The band gap for $Cd_{1-x}Zn_xS$ thin films can be tuned nonlinearly with x from about 2.38 eV for CdS to 3.74 eV for ZnS. A novel structure for $CuInS_2$-based solar cells with a $Cd_{0.4}Zn_{0.6}S$ layer is proposed in this paper.

1. Introduction

ZnS-based II-VI materials can form ternary alloys, such as $Cd_{1-x}Zn_xS$, with a direct fundamental band-gap range from 2.4 to 3.7 eV at room temperature. The energy position of the conduction band is changed primarily by varying the Zn content. Therefore, these materials have potential applications for efficient electron-confined structures, photovoltaic heterojunction, and electro-optical devices.

In photovoltaic system, the replacement of CdS with the higher band-gap $Cd_{1-x}Zn_xS$ has led to a decrease in window absorption losses and has resulted in an increase in the short-circuit current [1]. This $Cd_{1-x}Zn_xS$ ternary compound is also a useful buffer material for fabrication of *p-n* junctions without lattice mismatch [2].

$Cd_{1-x}Zn_xS$ thin films have been prepared by different techniques, which include evaporation [2–5], chemical bath deposition [1, 6, 7], and organic vapor deposition [8]. However, very little information is available on the ternary $Cd_{1-x}Zn_xS$ alloy films with the desired composition prepared by the vacuum evaporation technique. $Cd_{1-x}Zn_xS$ thin films, to our best knowledge, have been prepared by vacuum evaporation involved with three methods, one of which is the thin films being prepared by using a mechanically alloyed mixture of CdS and ZnS [3]. It is obvious that a homogenous mixture of $Cd_{1-x}Zn_xS$ is difficult to obtain. So Kumar et al. [4] synthesized the fine powders of $Cd_{1-x}Zn_xS$ by solid-state reaction and then deposited $Cd_{1-x}Zn_xS$ thin films. Considering the large difference in the vapor pressures of CdS and ZnS, Torres and Gordillo [5] prepared $Cd_{1-x}Zn_xS$ thin films by evaporation, varying the diameter of the openings of the coaxial chambers which contain the CdS and ZnS precursors. However, homogenous $Cd_{1-x}Zn_xS$ thin films with desired content are not readily deposited by the evaporation mentioned above. In this work, $Cd_{1-x}Zn_xS$ ($0 \leq x \leq 1$) thin films have been prepared by using a coevaporation of CdS and ZnS from two horizontal sources, which allows independent control of the temperature and consequently control of the partial vapor pressures of both precursors. The structural, compositional, optical properties have been investigated.

2. Experimental Details

$Cd_{1-x}Zn_xS$ thin films were deposited by the vacuum coevaporation technique, as described elsewhere [9], to a thickness of ~300 nm at room temperature. The vacuum system had a base pressure of 10^{-4} Pa and was partitioned into two

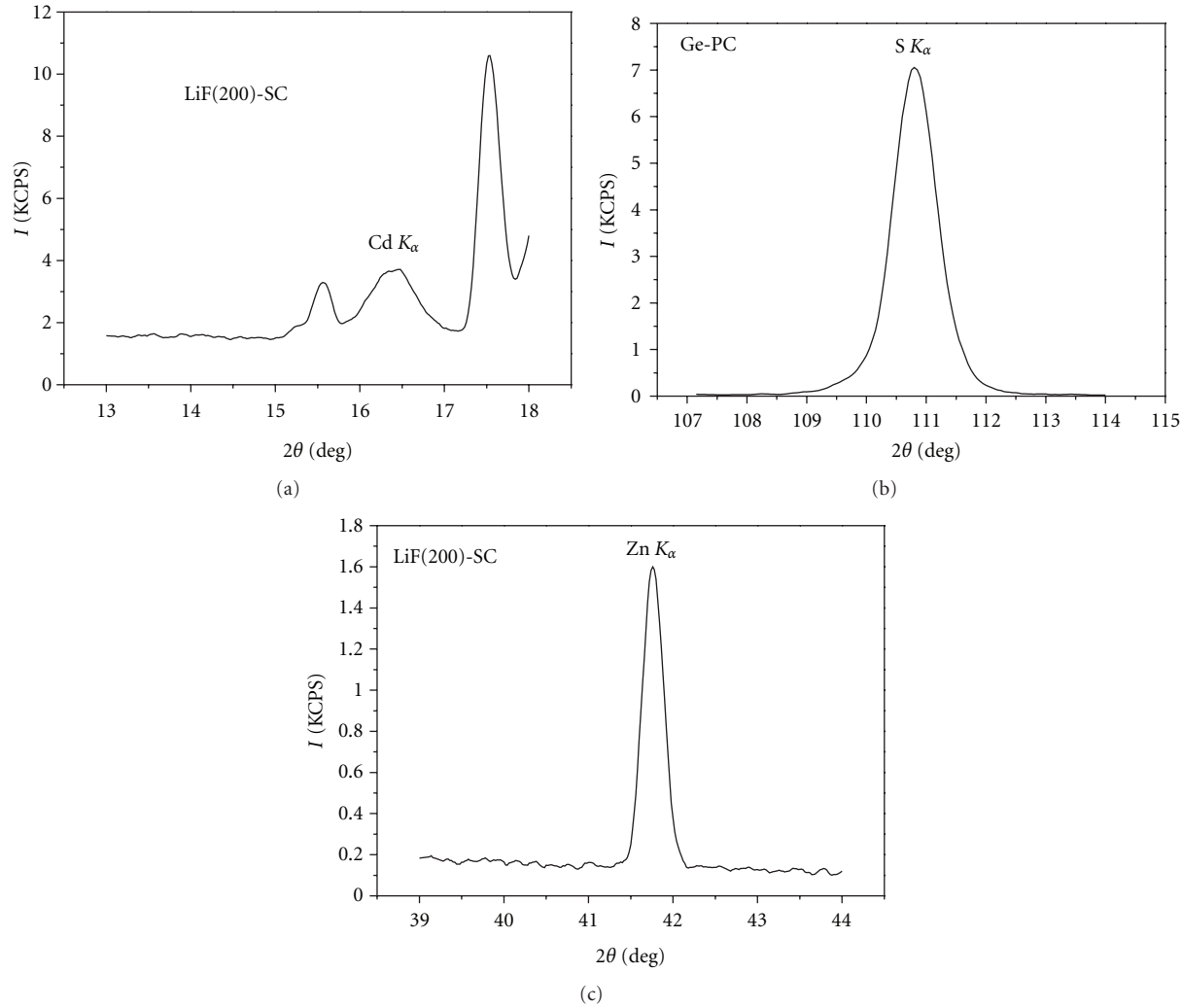

Figure 1: Typical XRF of $Cd_{1-x}Zn_xS$ ($x = 0.61$) thin films. (a) Cd-K_α, (b) S-K_α, and (c) Zn-K_α.

parts, one for a CdS powder source (5 N purity) and the other for a ZnS powder source (5 N purity). The CdS and ZnS deposition rates were measured by separate LHC-2 quartz monitors. The deposition rate of ZnS was adjusted to obtain different Zn concentrations in CdS thin films, varying between 0 and 1. The thickness was confirmed precisely by a surface profilometer. X-ray fluorescence (XRF) spectrometry was subsequently used to determine the composition of each sample. The crystallographic phase and lattice constants of each film were obtained by X-ray diffraction (XRD). Measurements of the optical transmittance were made over the wavelength range 200 $\sim$ 800 nm with a data interval of 0.5 nm. Transmittance measurements were also made with the beam at near-normal incidence to the sample to prevent reflected light being returned to the monochromator.

3. Results and Discussion

To accurately determine the composition of the $Cd_{1-x}Zn_xS$ alloys, X-ray fluorescence measurements of $Cd_{1-x}Zn_xS$ thin films were also carried out (Figure 1). Table 1 shows composition of the $Cd_{1-x}Zn_xS$ thin films from XRF using the fundamental parameter (FP) method.

Figure 2 demonstrates X-ray diffraction spectra of $Cd_{1-x}Zn_xS$ ($0 \leqslant x \leqslant 1$) thin films obtained by using Cu K_α radiation, where only one diffraction peak with a 2θ value between 26.38 and 28.37^0 is present. The absence of diffraction peaks associated with CdS and ZnS suggests that those thin films are single-phase materials. The presence of sharp peaks in XRD patterns demonstrates the polycrystalline nature of these $Cd_{1-x}Zn_xS$ ($0 \leqslant x \leqslant 1$) thin films, which have a strong preferential orientation. From XRD patterns, one can see that the diffraction angle (2θ) shifts towards a slightly higher angle with increasing x (Zn content) in the thin films. This is due to the substitution of Zn^{2+} for Cd^{2+}, in which different ionic radius of Cd^{2+} (0.095 nm) and Zn^{2+} (0.074 nm) [10] leads to the increase of lattice constants of $Cd_{1-x}Zn_xS$ thin films. Figure 2 also shows that the intensity of XRD peaks decreases at higher concentration of Zn. The structure of $Cd_{1-x}Zn_xS$ thin films varies continuously from being cubic zincblende material with a preferred

Table 1: Composition of $Cd_{1-x}Zn_xS$ thin films.

	No. 1	No. 2	No. 3	No. 4	No. 5
From XRF	$CdS_{0.93}$	$Cd_{0.72}Zn_{0.28}S$	$Cd_{0.59}Zn_{0.61}S$	$Cd_{0.11}Zn_{0.89}S$	$ZnS_{1.12}$
From Vegard's law	CdS	$Cd_{0.723}Zn_{0.277}S$	$Cd_{0.42}Zn_{0.58}S$	$Cd_{0.1}Zn_{0.9}S$	ZnS
From monitors	CdS	$Cd_{0.7}Zn_{0.3}S$	$Cd_{0.4}Zn_{0.6}S$	$Cd_{0.1}Zn_{0.9}S$	ZnS

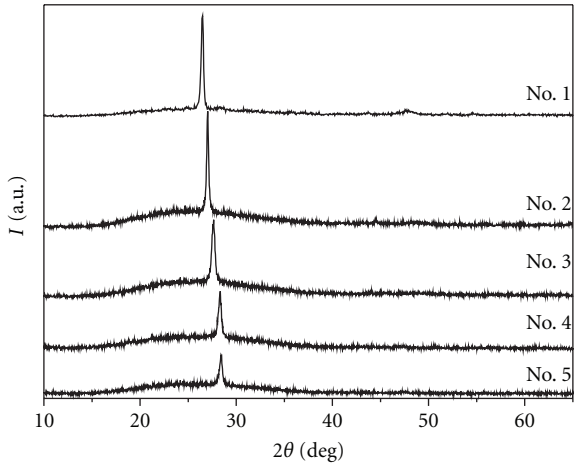

Figure 2: XRD patterns of as-deposited polycrystalline $Cd_{1-x}Zn_xS$ thin films.

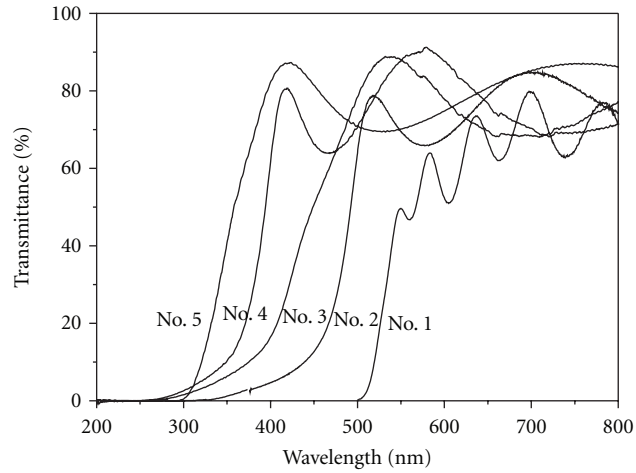

Figure 3: UV-visible transmission spectra of $Cd_{1-x}Zn_xS$ films.

orientation of (111) plane at the ZnS end to being hexagonal wurtzite with a preferential orientation of (002) plane when zinc content decreased.

Since the lattice constant of $Cd_{1-x}Zn_xS$ thin films follows Vegard's law, the composition of $Cd_{1-x}Zn_xS$ thin films can be determined by

$$x_{Cd_{1-x}Zn_xS} = \frac{a_{Cd_{1-x}Zn_xS} - a_{CdS}}{a_{ZnS} - a_{CdS}} \times 100\%, \quad (1)$$

where $a_{Cd_{1-x}Zn_xS}$, a_{CdS}, and a_{ZnS} are, respectively, the lattice constants of $Cd_{1-x}Zn_xS$, CdS, and ZnS. From the d values of the X-ray diffraction spectra shown in Figure 2 the lattice constants can be calculated as follows:

$$d = \frac{a}{\sqrt{(4/3)(h^2 + hk + k^2) + (a/c)^2 l^2}}. \quad (2)$$

Therefore, from (1) and (2), one can obtain the composition of $Cd_{1-x}Zn_xS$ thin films as shown in Table 1. It can be seen that there is a good agreement among the three sets of x values. As for the low angle diffraction line the variation of the diffraction angle with the composition is small and the determined film composition is not so accurate. The error is estimated to be about 0.05 in x. The precision suggests that we can control the composition of $Cd_{1-x}Zn_xS$ thin films, which are prepared by coevaporation of CdS and ZnS. In addition, the comparison of calculated d values from the diffraction spectra (Figure 2) with the standard d^* values from the JCPDS XRD spectra data for $Cd_{1-x}Zn_xS$ is shown in Table 2.

The optical transmittance spectra of the $Cd_{1-x}Zn_xS$ films with different x values were obtained, and steep absorption edges were observed, demonstrating that the thin films are homogeneous (Figure 3). The optical transmittance of the $Cd_{1-x}Zn_xS$ films is typically 60% at wavelengths beyond the absorption edge. It can be seen that $Cd_{1-x}Zn_xS$ films show the blue shift in the absorption edge with the increase of the zinc content.

From the transmittance curves of Figure 3, the absorption coefficient α of the thin films is estimated. The absorption coefficient α with the energy of the photon $h\upsilon$ could be expressed by the following equation:

$$\alpha h\upsilon \propto \left(h\upsilon - E_g\right)^m, \quad (3)$$

where E_g is the optical band gap of the thin films, and the exponent m may take values, $1, 2, 3, 1/2, 3/2$, depending on the electronic transitions in k-space. A linear fit is achieved for the $Cd_{1-x}Zn_xS$ films with $m = 1/2$, indicating that this material is a direct gap semiconductor. So $(\alpha h\upsilon)^2$ is plotted as a function of $h\upsilon$ for various zinc content (not shown there). The optical band energy gap can be determined from the intercept of the extrapolation of the straight portion to the $h\upsilon$ axis.

The band-gap dependence on composition is shown in Figure 4. It can be seen that the band gap varies with Zn content in a nonlinear way. This dependence can be determined by fitting the band-gap values to a parabolic form on the method of least square [11] and described as

$$E_g(x) = 2.38 + 0.69x + 0.67x^2. \quad (4)$$

It gives the bowing parameter (b) of 0.67 eV, which is much smaller than that reported on another $Cd_{1-x}Zn_xS$ alloy

Table 2: XRD results for $Cd_{1-x}Zn_xS$ thin films.

$Cd_{1-x}Zn_xS$	2θ	d	d^*	(hkl)	JCPDS
$x = 0$	26.442	3.3621	3.367	(002)	65–3414
$x = 0.28$	26.993	3.2972	3.290	(002)	40–0836
$x = 0.61$	27.613	3.2237	3.214[a]	(002)	—
$x = 0.89$	28.347	3.1480	3.142[a]	(002)	—
$x = 1$	28.533	3.1257	3.124	(111)	65–1691

[a] Calculated from Vegard's law.

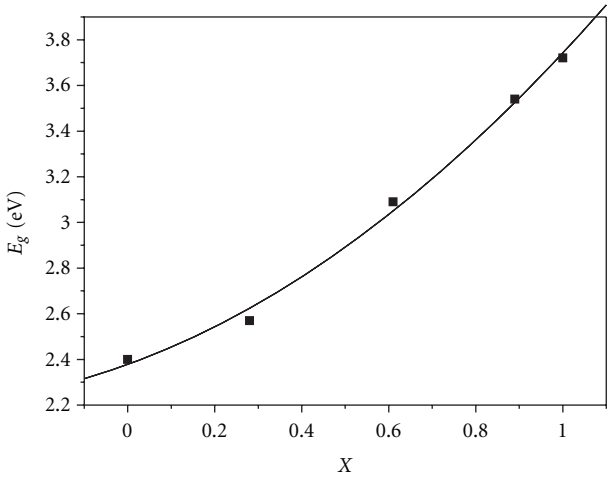

Figure 4: The variation of energy gap of the $Cd_{1-x}Zn_xS$ as a function of x.

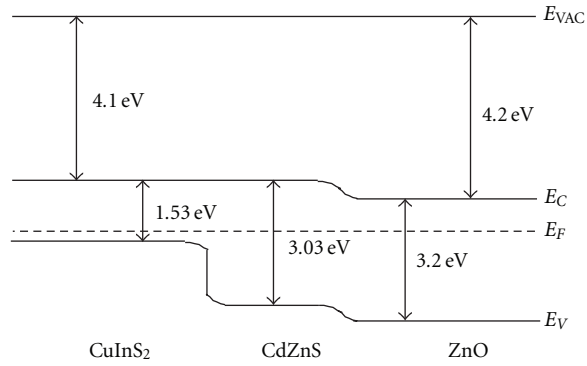

Figure 5: Flat band diagram of a $CuInS_2$/ZnO heterojunction with a $Cd_{0.4}Zn_{0.6}S$ buffer layer.

system in thin films by Borse et al. [6] ($b = 0.85$ eV) and that in single crystal by Muhamad [12] ($b = 0.82$ eV), but agrees well with that in thin films by Yamaguchi et al. [1] ($b = 0.724$ eV). In the present case of $Cd_{1-x}Zn_xS$ thin films, E_g values vary from 2.38 to 3.74 eV for $x = 0$ to 1 in a nonlinear way. This change in the band gap of CdS by addition of Zn shows formation of a continuous series of solid solutions. Therefore, the band energy gap of $Cd_{1-x}Zn_xS$ can be adjusted in the range of the binary band gaps. And the energy position of the conduction band, that is, electron affinity χ, can be also adjusted by varying the zinc content [2].

For the photovoltaic solar cells, $CuInS_2$ has a desirable direct band gap of 1.5 eV, which is also well-matched with the solar spectrum. Efficiency of 11.4% for $CuInS_2$-based solar cells has been successfully made [13]. However, further improvements on performance of $CuInS_2$-based solar cells have been restricted by the conventional structure due to the lattice mismatch between ZnO and $CuInS_2$. Therefore, an approach to overcome this problem is to introduce an effective buffer layer, $Cd_{1-x}Zn_xS$, in $CuInS_2$-based solar cells.

Furthermore, according to Anderson's model, the band alignments with $\chi_{\text{absorber}} \leqslant \chi_{\text{buffer}} \leqslant \chi_{\text{window}}$ are desired to prevent the formation of a conduction band spike in the $CuInS_2$-based solar cells. For Cu-rich films, electron affinity for $CuInS_2$ thin films is about 4.1 eV ($E_g \sim 1.53$ eV) [14, 15], and for ZnO thin films is about 4.2 eV ($E_g \sim 3.2$ eV), so the electron affinity of 4.1 eV for $Cd_{1-x}Zn_xS$ thin films (i.e., $x = 0.6$) [2] is taken into account. Based on these mentioned above, we propose a modified structure of $CuInS_2$-based solar cells. The energy band diagram of $CuInS_2$-based solar cells is shown in Figure 5. $Cd_{0.4}Zn_{0.6}S$ thin films ($E_g \sim 3.03$ eV, from (4)) provide lattice constant matching to the absorber and reduce the interface state density between the p- and n-type materials, meanwhile, the conduction band and valence band spikes are eliminated too.

4. Conclusions

$Cd_{1-x}Zn_xS$ thin films with the required composition have been successfully deposited on glass substrates by the vacuum coevaporation method. The thin films are found to be cubic at the ZnS end and hexagonal for $x < 1$, which show the highly preferred orientation. The measurements of optical transmittance for $Cd_{1-x}Zn_xS$ films demonstrate the blue shift in the absorption edge, and the optical band gap increases from 2.38 to 3.74 eV in a nonlinear way as composition varies from $x = 0$ to 1. And the energy position of the conduction band can be tuned by varying the zinc content. Therefore, a buffer layer $Cd_{1-x}Zn_xS$ for $x = 0.6$ is introduced in the $CuInS_2$-based solar cells to eliminate band spikes and provide lattice matching to the absorber.

Acknowledgments

Financial support from the National Basic Research Program of China (Grant no. 2011CBA007008), National Natural Science Foundation of China (Grant no. 61076058), and the Science and Technology Program of Sichuan Province, China (Grant no. 2008GZ0027) is gratefully acknowledged.

The authors thank Ms. Huiqin Sun, Analytical and Testing Center, Sichuan University, for optical transmittance spectra measurements.

References

[1] T. Yamaguchi, Y. Yamamoto, T. Tanaka, and A. Yoshida, "Preparation and characterization of (Cd,Zn)S thin films by chemical bath deposition for photovoltaic devices," *Thin Solid Films*, vol. 343-344, no. 1-2, pp. 516–519, 1999.

[2] R. Menner, B. Dimmler, R. H. Mauch, and H. W. Schock, "II-VI compound thin films for windows in heterojunction solar cells," *Journal of Crystal Growth*, vol. 86, no. 1–4, pp. 906–911, 1990.

[3] D. Patidar, N. S. Saxena, and T. P. Sharma, "Structural, optical and electrical properties of CdZnS thin films," *Journal of Modern Optics*, vol. 55, no. 1, pp. 79–88, 2008.

[4] P. Kumar, A. Misra, D. Kumar, N. Dhama, T. P. Sharma, and P. N. Dixit, "Structural and optical properties of vacuum evaporated $Cd_xZn_{1-x}S$ thin films," *Optical Materials*, vol. 27, no. 2, pp. 261–264, 2004.

[5] J. Torres and G. Gordillo, "Photoconductors based on $Zn_xCd_{1-x}S$ and $CdSe_{1-y}S_y$ thin films, fabricated with multilayer structure," *Thin Solid Films*, vol. 310, no. 1-2, pp. 310–316, 1997.

[6] S. V. Borse, S. D. Chavhan, and R. Sharma, "Growth, structural and optical properties of $Cd_{1-x}Zn_xS$ alloy thin films grown by solution growth technique (SGT)," *Journal of Alloys and Compounds*, vol. 436, no. 1-2, pp. 407–414, 2007.

[7] G. K. Padam, G. L. Malhotra, and S. U. M. Rao, "Studies on solution-grown thin films of $Zn_xCd_{1-x}S$," *Journal of Applied Physics*, vol. 63, no. 3, pp. 770–774, 1988.

[8] S. Yamaga, A. Yoshikawa, and H. Kasai, "Growth and properties of $Zn_{1-x}Cd_xS$ films on GaAs by low-pressure MOVPE," *Journal of Crystal Growth*, vol. 99, no. 1–4, pp. 432–436, 1990.

[9] W. Li, L. H. Feng, L. L. Wu et al., "Preparation and properties of polycrystalline CdS_xTe_{1-x} thin films for solar cells," *Wuli Xuebao/Acta Physica Sinica*, vol. 54, no. 4, pp. 1879–1884, 2005.

[10] R. D. Shannon, "Revised effective ionic radii and systematic studies of interatomic distances in halides and chalcogenides," *Acta Crystallographica Section A*, vol. 32, pp. 751–767, 1976.

[11] R. Hill, "Energy-gap variations in semiconductor alloys," *Journal of Physics C*, vol. 7, no. 3, article 009, pp. 521–526, 1974.

[12] M. R. Muhamad, "Excitonic electroabsorption in solid solution of $Cd_xZn_{1-x}S$ single crystals," *Japanese Journal of Applied Physics, Part 1*, vol. 32, no. 8, pp. 3385–3390, 1993.

[13] D. Braunger, D. Hariskos, T. Walter, and H. W. Schock, "An 11.4% efficient polycrystalline thin film solar cell based on $CuInS_2$ with a Cd-free buffer layer," *Solar Energy Materials and Solar Cells*, vol. 40, no. 2, pp. 97–102, 1996.

[14] R. Hunger, C. Pettenkofer, and R. Scheer, "Surface properties of (111), (001), and (110)-oriented epitaxial $CuInS_2$/Si films," *Surface Science*, vol. 477, no. 1, pp. 76–93, 2001.

[15] J. L. Lin, J. T. Lue, M. H. Yang, and H. L. Hwang, "Pulsed electron beam annealing of phosphorus-implanted $CuInS_2$," *Applied Physics Letters*, vol. 48, no. 16, pp. 1057–1059, 1986.